



Title	Generation of alkali-free and high-proton concentration layer in a soda lime glass using non-contact corona discharge
Author(s)	Ikeda, Hiroshi; Sakai, Daisuke; Funatsu, Shiro; Yamamoto, Kiyoshi; Suzuki, Toshio; Harada, Kenji; Nishii, Junji
Citation	Journal of Applied Physics, 114(6), 063303-1-063303-6 https://doi.org/10.1063/1.4817760
Issue Date	2013-08-14
Doc URL	http://hdl.handle.net/2115/53295
Rights	Copyright 2013 American Institute of Physics. This article may be downloaded for personal use only. Any other use requires prior permission of the author and the American Institute of Physics. The following article appeared in J. Appl. Phys. 114, 063303 (2013) and may be found at http://jap.aip.org/resource/1/japiau/v114/i6/p063303_s1
Type	article
File Information	JApplPhys_114_063303.pdf



[Instructions for use](#)

Generation of alkali-free and high-proton concentration layer in a soda lime glass using non-contact corona discharge

Hiroshi Ikeda, Daisuke Sakai, Shiro Funatsu, Kiyoshi Yamamoto, Toshio Suzuki et al.

Citation: *J. Appl. Phys.* **114**, 063303 (2013); doi: 10.1063/1.4817760

View online: <http://dx.doi.org/10.1063/1.4817760>

View Table of Contents: <http://jap.aip.org/resource/1/JAPIAU/v114/i6>

Published by the [AIP Publishing LLC](#).

Additional information on *J. Appl. Phys.*

Journal Homepage: <http://jap.aip.org/>

Journal Information: http://jap.aip.org/about/about_the_journal

Top downloads: http://jap.aip.org/features/most_downloaded

Information for Authors: <http://jap.aip.org/authors>



Generation of alkali-free and high-proton concentration layer in a soda lime glass using non-contact corona discharge

Hiroshi Ikeda,^{1,a)} Daisuke Sakai,¹ Shiro Funatsu,² Kiyoshi Yamamoto,³ Toshio Suzuki,³ Kenji Harada,⁴ and Junji Nishii¹

¹Research Institute for Electronic Science, Hokkaido University, N20 W10, Kita-ku, Sapporo, Hokkaido 001-0020, Japan

²Production Technology Center, Asahi Glass Co., Ltd., 1-1 Suehiro-cyo, Tsurumiku, Yokohama, Kanagawa 230-0045, Japan

³Research Center, Asahi Glass Co., Ltd., 1150 Hazawa-cho, Kanagawa-ku, Yokohama, Kanagawa 221-8755, Japan

⁴Department of Computer Science, Kitami Institute of Technology, 165 Koen-cho, Kitami, Hokkaido 090-8507, Japan

(Received 7 June 2013; accepted 23 July 2013; published online 8 August 2013)

Formation mechanisms of alkali-free and high-proton concentration surfaces were investigated for a soda lime glass using a corona discharge treatment under an atmospheric pressure. Protons produced by high DC voltage around an anode needle electrode were incorporated into a sodium ion site in the anode side glass. The sodium ion was swept away to the cathode side as a charge carrier. Then it was discharged. The precipitated sodium was transformed to a Na_2CO_3 powder when the surface contacted with air. The sodium ion in the glass surface layer of the anode side was replaced completely by protons. The concentration of OH groups in the layer was balanced with the amount of excluded sodium ions. The substitution reaction of sodium ions with protons tends to be saturated according to a square root function of time. The alkali depletion layer formation rate was affected by the large difference in mobility between sodium ions and protons in the glass. © 2013 AIP Publishing LLC. [<http://dx.doi.org/10.1063/1.4817760>]

I. INTRODUCTION

Several modification techniques have been developed for glass surfaces, such as ion implantation method,¹ ion-exchange using a molten salt,² and heat-treatment in an active gas.³ An externally applied DC voltage also attracts great interest as a modification method. For example, thermal poling, which applies high voltage across the electrodes to a glass with heat treatment, generates an alkali depletion area, including structural defects in the glass, leading to second harmonic generation, and the electro-optical effect.⁴⁻¹⁰ Recently, electro-field imprint processing, which is an imprint technique assisted by DC voltage applied between the molds,¹¹⁻¹⁴ has been studied for the fabrication of plasmonic microstructures on the surface of a metal-glass composite material. Corona discharge has been identified as a useful non-contact surface modification method for several materials.¹⁵⁻²¹ The corona is a non-disruptive electrical discharge created by application of a high DC voltage between an anode and a cathode. For example, a material surface on the plate cathode electrode is charged with ions generated around the anode needle electrode, leading to the generation of a large electric field on the material surface. Considerable effort has been devoted to corona discharge treatment for the surface modification of dielectric polymers.^{15,16,21}

We previously recorded a hologram on the soda lime glass surface using the corona discharge treatment.²²⁻²⁶ Surface-relief gratings of an azobenzene polymer, which were fabricated on the glass surface using two-beam interference, were transferred onto the glass surface after the corona discharge treatment. The treatment conditions strongly affected the diffraction efficiency of the grating formed on the glass surface. However, the formation mechanism of such holographic grating remains ambiguous. This study was undertaken to elucidate the surface modification phenomena of soda lime glasses caused by the corona discharge treatment.

II. EXPERIMENTAL

A schematic set up of the corona discharge treatment is shown in Figure 1. A steel needle coated with Pt was used with a flat carbon plate, respectively, as anode and cathode electrodes. The anode electrode was connected to a DC power supply. The cathode electrode was grounded. The current in the circuit was monitored using a data logger (midi Logger GL220; Graphtec Corp.). Commercially available soda lime glass (AS; Asahi Glass Co. Ltd.) was used for the experiment. The sodium and calcium oxide contents were, respectively, 13 mol. % and 9 mol. %. The glass was polished using a colloidal silica compound to suppress the alkali dissolution from its surface during polishing. The glass plate of 25 mm × 25 mm × 1 mm was placed on the cathode plate. The distance between the needle and the glass surface was 5 mm. The corona discharge treatment was performed at temperatures between 100 °C and 400 °C in an atmosphere

^{a)}Author to whom correspondence should be addressed. Electronic mail: ikedah@astec.kyushu-u.ac.jp. Present address: Art, Science and Technology Center for Cooperative Research, Kyushu University, 6-1 Kasuga-koen, Kasuga, Fukuoka 816-8580, Japan.

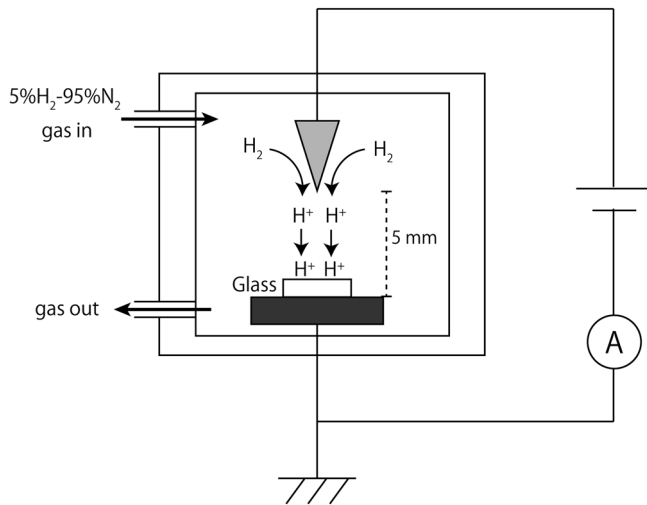


FIG. 1. Corona discharge setup for glass surface treatment. Anode and cathode electrodes are, respectively, a steel needle and a carbon plate. The needle size in the scheme is exaggerated.

of 5 vol. % H_2 and 95 vol. % N_2 . The applied voltage, which was controlled below the arc discharge level, was less than 7 kV for our setup. After treatment, the glass was cooled gradually to room temperature in the furnace.

Infrared (IR) absorption spectra of the treated glass were examined using a Fourier transform infrared absorption spectrometer (FT-IR, Affinity-1; Shimadzu Corp.). White compounds precipitated on the cathode side glass surface were dissolved in distilled water and were analyzed using inductive coupled plasma atomic emission spectroscopy (ICP-AES; ICPE-9000; Shimadzu Corp.). The depth profile of the glass composition was analyzed using energy dispersive X-ray spectroscopy (EDS; JED-2300; JEOL Ltd.).

III. RESULTS

Voltage–current (V–I) characteristics found during the corona discharge treatment at 100°C are shown in Figure 2. At voltages above the threshold of 3.8 kV, the corona

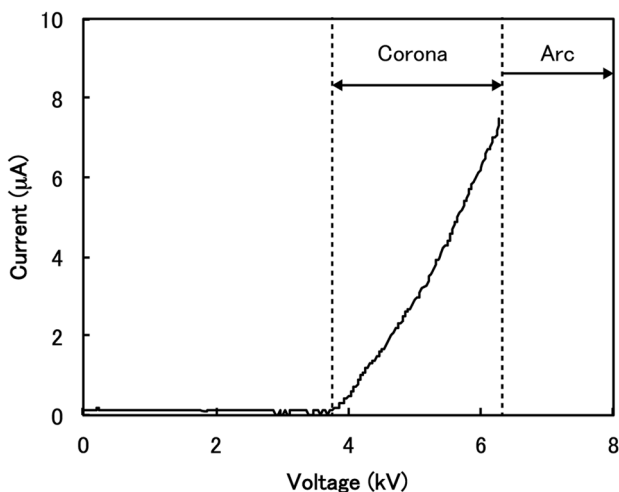


FIG. 2. Relation between applied voltage and current during corona discharge treatment on the soda lime glass surface at 100°C in a nitrogen atmosphere containing 5 vol. % H_2 .

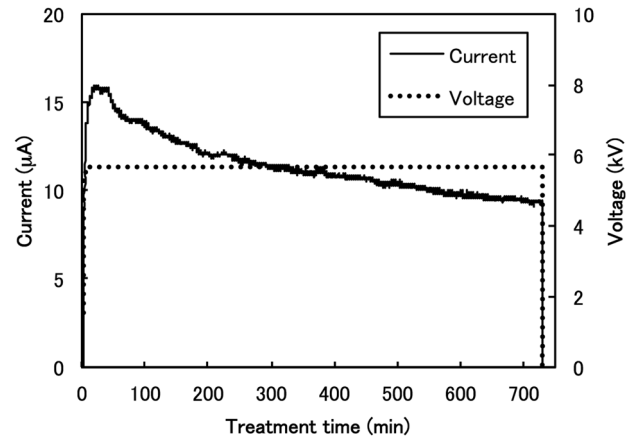


FIG. 3. Time dependence of current during corona discharge treatment on the soda lime glass at 100°C .

discharge occurred with the ionization of the gas molecules around the anode needle, leading to the current flow, which increased gradually with the applied voltage. When the applied voltage was too high, the corona discharge was transformed to the arc discharge, resulting in fatal surface sputtering damage. Figure 3 presents the time dependence of current during the treatment, which increased to $16\ \mu\text{A}$ with the voltage. It subsequently decreased gradually to $9\ \mu\text{A}$ after treatment for 720 min. The white precipitates confirmed on the anode side glass surface were identified as Na_2CO_3 using ICP-AES and Raman spectroscopy, which should be formed by the chemical reaction of the discharged sodium metal with air including CO_2 gas. The amount of the precipitate that had formed after treatment at 100°C was higher than those that formed at 200, 300, and 400°C .

Figure 4 shows the time dependence of the sodium precipitated after the corona discharge treatment at 100°C and the applied voltage of 5.7 kV. The amount of sodium increased with the treatment time, although no change was found in the precipitated area against the treatment time: it was 16 mm diameter. Figure 5 shows a cross-section optical view of the glass treated at 100°C with 5.7 kV for 720 min. An approximately $3\ \mu\text{m}$ thick layer was observed at the

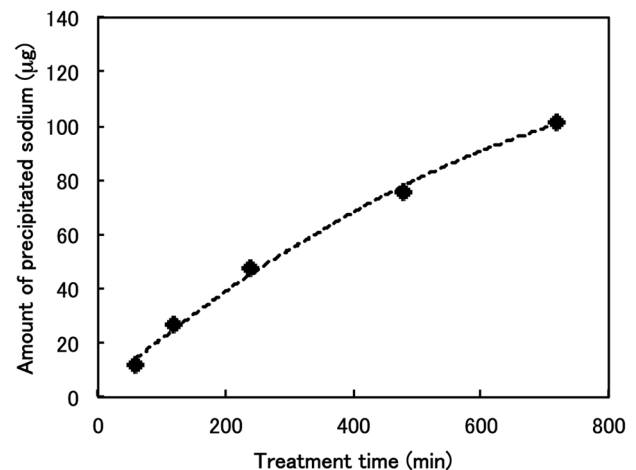


FIG. 4. Relation between corona discharge treatment time and precipitated sodium converted from the amount of Na_2CO_3 analyzed using ICP-AES.

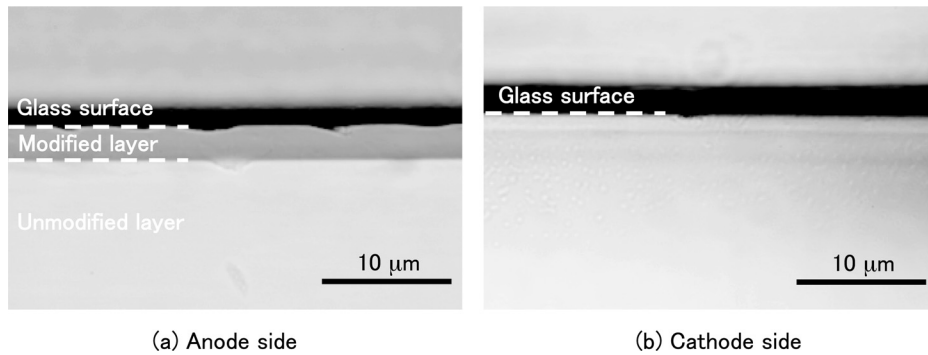


FIG. 5. Cross-sectional glass surface views after corona discharge treatment under applied voltage of 5.7 kV at 100 °C for 720 min: (a) anode side and (b) cathode side.

anode side glass surface. In contrast, no modified layer was found at the cathode side glass surface. The thin layer composition was analyzed using EDS. Figure 6 presents depth profiles of representative metals in the glass matrix. A step-like sodium depletion layer was confirmed at the anode side surface. The calculated amount of sodium ions in this layer agreed well with the precipitated sodium results obtained using ICP-AES analysis. These results demonstrate that the sodium ions in the glass drifted from the anode side to the cathode side as charge carriers; then they were discharged.

The IR absorption spectra of the glasses were measured before and after the corona discharge treatment. Significant differences were recognized in the wavelength range of 2500–3700 cm^{-1} . Figure 7 portrays spectra after the corona discharge treatment for 60–720 min. Broad peaks were assignable to OH groups.²⁷ These peak intensities increased with the treatment time. The OH group depth profiles were evaluated through careful polishing of the anode side surface. Figure 8 depicts the IR absorption spectra before and after eliminating the surface layer by approximately 10 μm . The peak intensities after polishing are apparently reduced to the same level as that of the untreated glass. Therefore, the OH groups that increased after the corona discharge treatment were located only at the sodium depletion layer.

IV. DISCUSSION

A. Substitution reaction of sodium ion with proton

The corona discharge treatment, respectively, induced the sodium depletion layer and the precipitation of Na_2CO_3 at the anode and cathode side surfaces. Furthermore, OH groups were formed in the sodium depletion layer. Therefore, it is evident that the charge carrier during the

treatment was sodium ions and that the protons were introduced to the sodium depletion layer as the charge compensator. All of these electrochemical phenomena are explained stoichiometrically as shown in Figure 9, which presents the time dependence of the electrical charges and the amount of precipitated sodium and incorporated OH groups by the corona discharge treatment at 100 °C. Each value was obtained using the following methods. (a) The electrical charges were estimated by the time integration of the current during corona discharge treatment using the Faraday constant of 96 485 C mol^{-1} . Here, the carrier is assumed to be only sodium ion. (b) The amount of the precipitated sodium was analyzed using the ICP-AES (see Figure 4). (c) The OH groups introduced by the corona discharge treatment were estimated from the IR absorption intensities in Figure 7 using the two-band method reported by Scholze.^{27,28} It is possible to calculate the amount of OH groups from the peaks at 2800 cm^{-1} and 3500 cm^{-1} in the IR absorption spectrum of a glass:

$$OH_{total} = \frac{V}{d} \left(\frac{\alpha_{3500}}{\epsilon_{3500}} + \frac{4}{3} \cdot \frac{\alpha_{2800}}{\epsilon_{2800}} \right). \quad (1)$$

In that equation, d stands for the thickness, V is the volume, and α_{2800} and α_{3500} , respectively, represent the absorption coefficients at 2800 cm^{-1} and 3500 cm^{-1} . The absorption coefficients of 164 $\text{l mol}^{-1}\text{cm}^{-1}$ and 76 $\text{l mol}^{-1}\text{cm}^{-1}$ are used, respectively, for α_{2800} and α_{3500} . The thickness d is 1 mm. Volume V is determined from the glass thickness and the corona discharged circle area of 16 mm diameter. As presented in Figure 9, the total electrical charges, the amounts of precipitated sodium and the total concentration of OH groups are increased linearly against the square root of the treatment time with a similar slope. Consequently, the

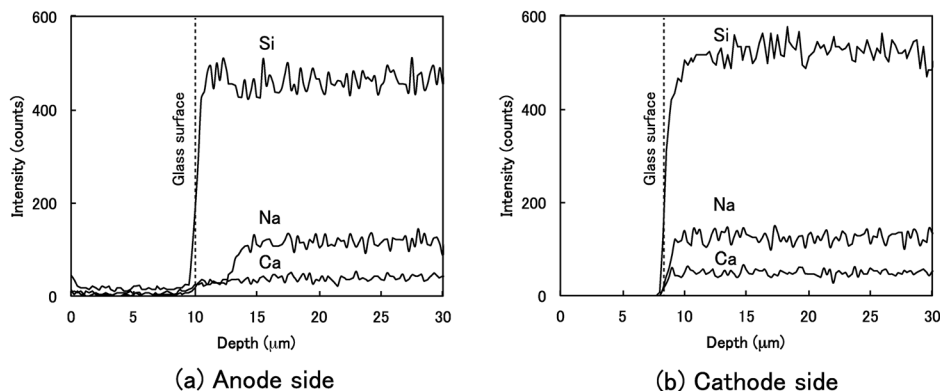


FIG. 6. Depth profile of representative cations for the specimen shown in Figure 5: (a) anode side and (b) cathode side.

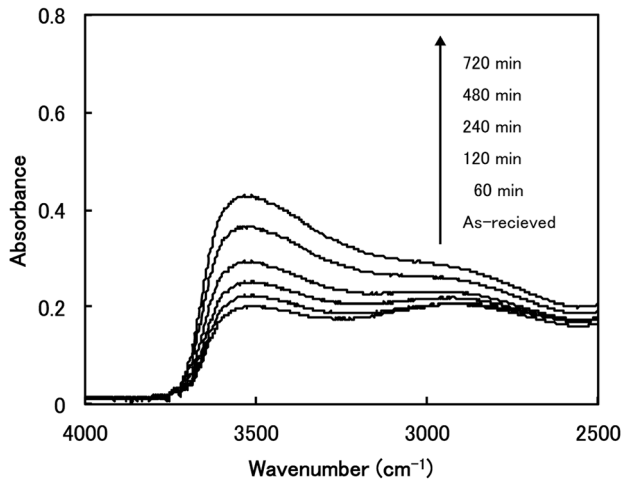
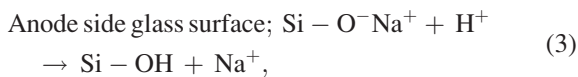
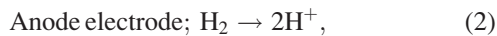


FIG. 7. IR absorption spectra of the soda lime glass after corona discharge treatment at 100 °C.

chemical reactions caused in the soda lime glass by the corona discharge treatment can be expressed as shown below:



Reactions (2), (3), and (4), respectively, show the ionization of the H_2 gas molecule caused by the large electric field at the anode needle electrode, the substitution of sodium ions with protons in the glass network, and the discharge of sodium ions to sodium atoms at the cathode side. The corona discharge in the hydrogen atmosphere generates not only H^+ , but also H_3^+ and H_5^+ .²⁹ In addition, if a small amount of H_2O exists in the ambient atmosphere, then $(\text{H}_2\text{O})_n\text{H}^+$ or other radical species are generated.³⁰ However, our results revealed that the one-on-one exchange of sodium ion to proton proceeded because the sodium ions were swept away

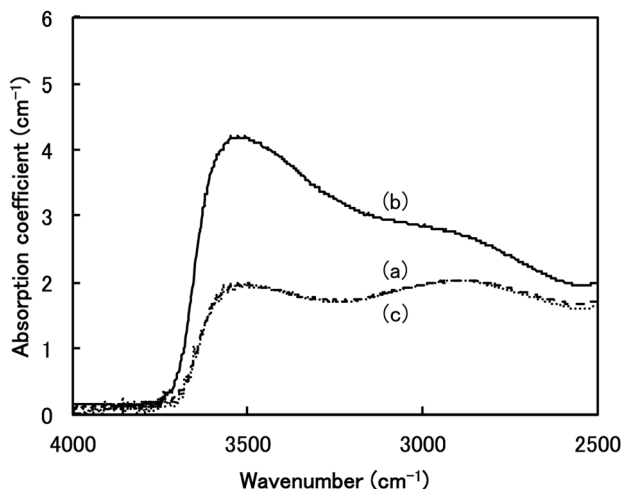


FIG. 8. IR absorption spectra (a) before and (b) after corona discharge treatment at 5.7 kV, 100 °C for 720 min. Spectrum (c) was obtained after eliminating the anode side surface of 10 μm by polishing.

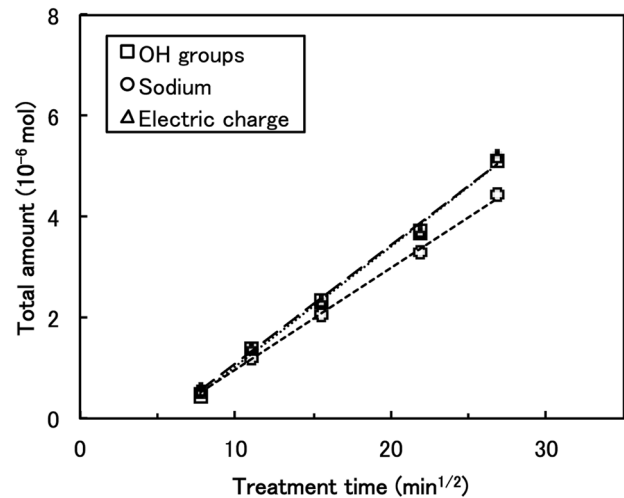


FIG. 9. Time dependence of (a) total electrical charge, (b) total precipitated sodium, and (c) OH concentration increased by the corona discharge treatment at 5.7 kV, 100 °C. These three amounts were estimated, respectively, from the measured current during the treatment, ICP-AES measurement and IR absorption spectra.

completely from the hydrogen injected layer and the total charge measured during the treatment agreed with the sodium ion concentration in the depletion layer. Therefore, the predominant ionization of gases can be written as $\text{H}_2 \rightarrow 2\text{H}^+$: the reaction (2).

B. Formation mechanism of sodium depletion layer

Figure 10 presents the time dependence of the sodium depletion layer thickness by the corona discharge treatment obtained from the amount of the precipitated sodium (Figure 4). The sodium depletion layer thickness was fitted by the theoretical model developed by Prieto and Linares to analyze the ion exchange process assisted by a DC electric field for an optical waveguide fabrication.³¹ The time dependence of the sodium depletion layer thickness $l(t)$ is expressed as follows:³¹

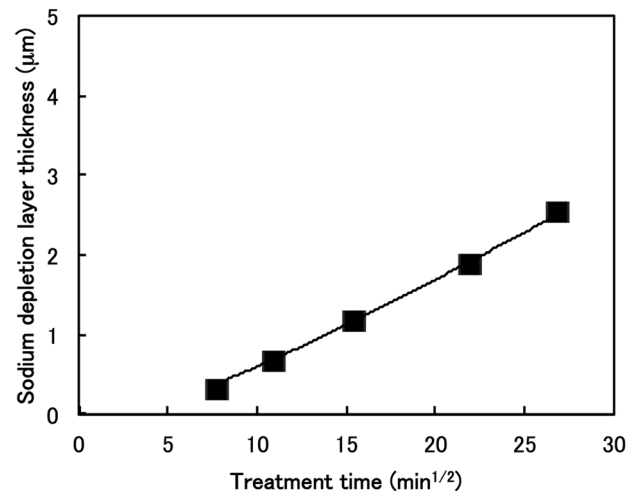


FIG. 10. Time dependence of the sodium depletion layer thickness by the corona discharge treatment at 5.7 kV, 100 °C. The closed square symbol was obtained using the amount of precipitated sodium (Figure 4) and solid line was obtained using Eq. (5).

TABLE I. Properties of a soda lime glass and experimental condition used for the calculation.

Glass thickness, L (mm)	Sodium concentration C_{Na} (mol m ⁻³)	H ⁺ mobility μ_H (m ² V ⁻¹ s ⁻¹) ^{a,32}	Na ⁺ mobility μ_{Na} (m ² V ⁻¹ s ⁻¹) ³⁷
1	1.0×10^4	7×10^{-19}	7×10^{-16}

^aThe Na⁺ mobility is 1000 times as high as the H⁺ mobility.

$$l(t) = \left(\frac{1}{\alpha N_H} - 1 \right) \left[\sqrt{\frac{2\alpha N_H \mu_H V}{(1-\alpha)^2} t + L^2} - L \right]. \quad (5)$$

In that equation, L stands for the glass thickness, V signifies the voltage across the glass, $\alpha = 1 + \mu_H/\mu_{Na}$ represents the ion-mismatched parameter, and μ_H and μ_{Na} , respectively, denote the mobilities of protons and sodium ions. $N_H = C_H/C_{Na}^0$, which is the ratio of proton concentration C_H to the intrinsic sodium ion concentration C_{Na}^0 , is assumed to be 1 because the sodium ions in the sodium depletion layer were exchanged completely to the protons. The values used for the calculation are presented in Table I. The calculated result agreed well with our experimentally obtained result. The sodium depletion layer thickness increased against the square root of time and the voltage across the glass V was calculated to 0.2 kV using Eq. (5). Considering that the total applied voltage was 5.7 kV in the corona discharge treatment, then presumably, 5.5 kV was consumed in the atmosphere to generate the protons that drifted onto the glass surface. As the results showed, we estimated the voltage V_{surf} and the electric field E_{surf} across the sodium depletion layer using the following equations, which can be derived from the equations in an earlier report.³¹

$$V_{surf}(t) = \frac{V}{\alpha} \left(1 - \frac{L}{\sqrt{\frac{2\alpha\mu_H V}{(1-\alpha)^2} t + L^2}} \right), \quad (6)$$

$$E_{surf}(t) = \frac{V}{(1-\alpha) \sqrt{\frac{2\alpha\mu_H V}{(1-\alpha)^2} t + L^2}}. \quad (7)$$

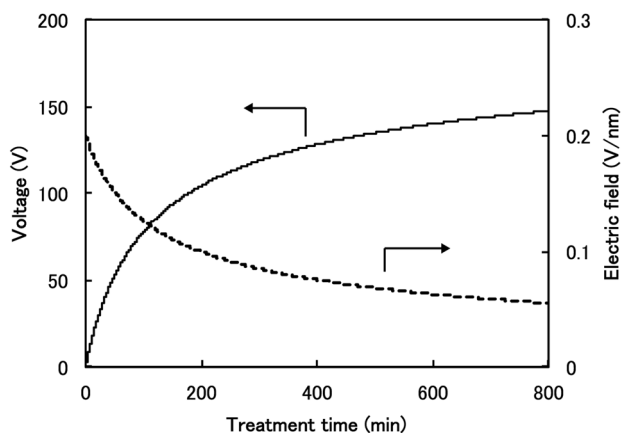


FIG. 11. Time dependence of voltage and electric field across the sodium depletion layer calculated, respectively, using Eqs. (6) and (7).

Figure 11 shows the calculated value for the voltage and the electric field across the sodium depletion layer during the corona discharge treatment using Eqs. (6) and (7). Results show that the large electric field was generated in the sodium depletion layer during the corona discharge treatment, which means that the electrical conductivity of the layer decreased significantly by the substitution of sodium ions with proton. Consequently, the voltage was concentrated in the thin layer. According to results of an earlier study,⁵ the conductivity of sodium depletion layer in a soda lime glass is comparable to that of a fused silica glass. Indeed, the mobility ratio (μ_{Na}/μ_H) of sodium ion (μ_{Na}) and proton (μ_H) in a soda lime glass was reported as of the order of 10^3 .^{32–34} Results suggest that formation of the sodium depletion layer resulted from the large difference of the mobilities between sodium ion and proton.

Studies on the thermal poling to a soda lime glass reported the formation of the alkali depletion layer on the anode side surface under the condition of several kilovolts at around 200 °C in air.^{32,35} However, the substitution of sodium ion with proton by this method proceeds only slightly, which is a discriminate point from the corona discharge treatment. Krieger and Lanford investigated the transport phenomena of ions (sodium, calcium ions, and proton) in a soda lime glass with application of DC voltage using Rutherford backscattering technique.³⁶ They used a “blocking electrode” to prevent the penetration of any ions, including proton to the glass from ambient air or the electrode. The results indicated that the sodium depletion layer thickness was about 300 nm after the treatment at 300 V and 150 °C over 60 h. In contrast, our results indicate thickness of 3 μm at 100 °C and 200 V (estimated voltage across the glass using Eq. (5)) for 12 h was reached. According to the previous study about thermal poling of the soda lime glass,³² the growth rate of the sodium depletion layer depends on the mobility of mobile ions, which are proton or oxygen ions, to compensate the sodium ion. The proton mobility is much greater than oxygen ion mobility. Therefore, the sodium depletion layer growth rate was increased by penetration of the proton from ambient atmosphere. During the corona discharge treatment, protons were introduced from the ambient atmosphere. Consequently the concentration of protons as OH groups in the sodium depletion layer reached the level of approximately 13 mol. %, which was comparable to the concentration of intrinsic sodium. Therefore, corona discharge treatment is expected to be useful for the non-contact substitution processing of alkali ion with protons for glasses and ceramics of several kinds.

V. CONCLUSION

Corona discharge was applied to soda lime glass at 100 °C in an atmosphere of 5 vol. % H₂ and 95 vol. % N₂. The substitution of sodium ions with protons proceeded at the anode side surface during the treatment. The sodium depletion layer thickness increased as a function of the square root of time. The theoretical model predicts that a large electric field should be applied on the anode side glass surface during the treatment. The layer thickness was

restricted by the mobility ratio of sodium ion and proton, which is in the order of 10^3 in the soda lime glasses. The non-contact corona discharge treatment is expected to be useful for the formation of alkali-free and high-proton concentration surface on glasses and ceramics under a low temperature with atmospheric pressure.

ACKNOWLEDGMENTS

This work was supported by Asahi Glass Co. Ltd.

- ¹G. W. Arnold, *J. Non-Cryst. Solids* **179**, 288 (1994).
- ²T. Pozzner, G. Schreiter, and R. Muller, *J. Appl. Phys.* **70**, 1966 (1991).
- ³S. Deriano, T. Rouxel, S. Malherbe, J. Rocherulle, G. Duisit, and G. Jezequel, *J. Eur. Ceram. Soc.* **24**, 2803 (2004).
- ⁴X. M. Liu and M. D. Zhang, *Jpn. J. Appl. Phys., Part 1* **40**, 4069 (2001).
- ⁵Y. Enami, P. Poyhonen, D. L. Mathine, A. Bashar, P. Madasamy, S. Honkanen, B. Kippelen, N. Peyghambarian, S. R. Marder, A. K. Y. Jen, and J. Wu, *Appl. Phys. Lett.* **76**, 1086 (2000).
- ⁶M. I. Petrov, A. V. Omelchenko, and A. A. Lipovskii, *J. Appl. Phys.* **109**, 094108 (2011).
- ⁷Y. T. Ren, C. J. Marckmann, J. Arentoft, and M. T. Kristensen, *IEEE Photon. Technol. Lett.* **14**, 639 (2002).
- ⁸N. J. Smith, M. T. Lanagan, and C. G. Pantano, *J. Appl. Phys.* **111**, 083519 (2012).
- ⁹A. Narazaki, K. Tanaka, K. Hirao, and N. Soga, *J. Am. Ceram. Soc.* **81**, 2735 (1998).
- ¹⁰A. L. Moura, M. T. de Araujo, E. A. Gouveia, M. V. D. Vermelho, and J. S. Aitchison, *Opt. Express* **15**, 143 (2007).
- ¹¹M. Leitner, H. Peterlik, B. Sepiol, H. Graener, M. Beileites, and G. Seifert, *Phys. Rev. B* **79**, 153408 (2009).
- ¹²A. Abdolvand, A. Podlipensky, S. Matthias, F. Syrowatka, U. Gosele, G. Seifert, and H. Graener, *Adv. Mater.* **17**, 2983 (2005).
- ¹³P. N. Brunkov, V. G. Melekhin, V. V. Goncharov, A. A. Lipovskii, and M. I. Petrov, *Tech. Phys. Lett.* **34**, 1030 (2008).
- ¹⁴A. A. Lipovskii, V. G. Melehin, M. I. Petrov, Y. P. Svirko, and V. V. Zhurikhina, *J. Appl. Phys.* **109**, 011101 (2011).
- ¹⁵H. J. Jung, Y. J. Park, S. H. Choi, J. M. Hong, J. Huh, J. H. Cho, J. H. Kim, and C. Park, *Langmuir* **23**, 2184 (2007).
- ¹⁶K. Munakata, K. Harada, H. Anji, M. Itoh, T. Yatagai, and S. Umegaki, *Opt. Lett.* **26**, 4 (2001).
- ¹⁷P. Cheben, F. del Monte, D. J. Worsfold, D. J. Carlsson, C. P. Grover, and J. D. Mackenzie, *Nature* **408**, 64 (2000).
- ¹⁸M. Stahelin, C. A. Walsh, D. M. Burland, R. D. Miller, R. J. Twieg, and W. Volksen, *J. Appl. Phys.* **73**, 8471 (1993).
- ¹⁹F. Chaput, D. Riehl, J. P. Boilot, K. Cargnelli, M. Canva, Y. Levy, and A. Brun, *Chem. Mater.* **8**, 312 (1996).
- ²⁰J. A. Giacometti and O. N. Oliveira, *IEEE Trans. Electr. Insul.* **27**, 924 (1992).
- ²¹J. A. Giacometti, P. A. Ribeiro, M. Raposo, J. N. Maratmendes, J. S. C. Campos, and A. S. Dereggi, *J. Appl. Phys.* **78**, 5597 (1995).
- ²²D. Sakai, K. Harada, S. Kamemaru, and T. Fukuda, *Appl. Phys. Lett.* **90**, 061102 (2007).
- ²³D. Sakai, K. Harada, S. Kamemaru, D. Barada, F. Sato, and T. Fukuda, *Jpn. J. Appl. Phys. Part 1* **47**, 7929 (2008).
- ²⁴D. Sakai, D. Miho, K. Harada, D. Barada, and T. Fukuda, *Jpn. J. Appl. Phys. Part 1* **49**, 01AE01 (2010).
- ²⁵D. Sakai, K. Harada, S. Kamemaru, D. Barada, F. Sato, and T. Fukuda, *Opt. Rev.* **16**, 335 (2009).
- ²⁶D. Sakai, K. Harada, S. Kamemaru, and T. Fukuda, *Opt. Rev.* **14**, 339 (2007).
- ²⁷H. Behrens and A. Stuke, *Glass Sci. Technol.* **76**, 176 (2003).
- ²⁸U. Harder and H. Geissler, *Fresenius' J. Anal. Chem.* **361**, 585 (1998).
- ²⁹D. J. Mellor and J. R. Travis, *J. Phys. D: Appl. Phys.* **5**, 1117 (1972).
- ³⁰M. M. Shahin, *J. Chem. Phys.* **45**, 2600 (1966).
- ³¹X. Prieto and J. Linares, *Opt. Lett.* **21**, 1363 (1996).
- ³²M. Dussauze, V. Rodriguez, A. Lipovskii, M. Petrov, C. Smith, K. Richardson, T. Cardinal, E. Fargin, and E. I. Kamitsos, *J. Phys. Chem. C* **114**, 12754 (2010).
- ³³G. Hetherington, K. H. Jack, and M. W. Ramsay, *Phys. Chem. Glasses* **6**, 6 (1965).
- ³⁴W. A. Lanford, K. Davis, P. Lamarche, T. Laursen, R. Groleau, and R. H. Doremus, *J. Non-Cryst. Solids* **33**, 249 (1979).
- ³⁵E. C. Ziemath, V. D. Araujo, and C. A. Escanhoela, *J. Appl. Phys.* **104**, 054912 (2008).
- ³⁶U. K. Krieger and W. A. Lanford, *J. Non-Cryst. Solids* **102**, 50 (1988).
- ³⁷C. M. Lepienski, J. A. Giacometti, G. F. L. Ferreira, F. L. Freire, and C. A. Achete, *J. Non-Cryst. Solids* **159**, 204 (1993).